

Effects of Welding Parameters of Pulsed Gas Metal Arc Welding on Microstructure and Mechanical Performance of Joints Welded in Hyperbaric Environment



Songtao Huang, Yongming Zhang, Xiangdong Jiao, Canfeng Zhou*

Beijing Higher Institution Engineering Research Center of Energy Engineering Advanced Joining Technology, Beijing
Institute of Petrochemical Technology, Beijing 102617, China

Corresponding Author Email: canfeng@bipt.edu.cn

<https://doi.org/10.18280/acsm.440408>

ABSTRACT

Received: 8 May 2020

Accepted: 29 July 2020

Keywords:

pulsed gas metal arc welding (GMAW), hyperbaric environment, arc voltage, pulse frequency, microstructure, mechanical performance

Hyperbaric welding is an important underwater repair technology for offshore structures. This paper mainly explores the effects of welding parameters (e.g. arc voltage, base current, peak current, and pulse frequency) of pulsed gas metal arc welding (GMAW) on the formation, microstructure, and mechanical performance of joints welded under hyperbaric environment. Firstly, a hyperbaric welding test system was designed simulate the repair of subsea structures. Next, multiple specimens were prepared for welding tests, tensile tests and Charpy impact tests. During the welding tests, only one welding parameter was adjusted at a time, aiming to disclose the influence of that specific parameter on weld formation, and the microstructure and mechanical performance of weld zone and heat affected zone (HAZ). The results show that: Ambient pressure greatly suppresses the arc behavior, weld formation, and weld quality. The suppression could be effectively compensated for by elevating the arc voltage. The microstructures of weld zone and HAZ could be changed in varied degrees by adjusting welding parameters of GMAW, including arc voltage, peak current, base current, and pulse frequency. Ambient pressure also affects the mechanical performance of welding joints in terms of tensile strength, Vickers hardness and toughness. The mechanical performance could be improved by adjusting the welding parameters. The research results provide important guidance for the repair of underwater structures like steel structures on oil platform and subsea pipelines.

1. INTRODUCTION

Underwater welding is a key technique in the repair of underwater structures, such as steel structures on oil platform and subsea pipelines [1]. Common underwater welding methods include friction welding (FRW) [2], gas tungsten arc welding (GTAW), and gas metal arc welding (GMAW).

FRW machines driven by hydraulic fluid can operate directly in water, and adapt to deep water environment. But these machines only support special operations like replacing anode stud [3]. GTAW is widely recognized for its high welding quality. If the water is shallower than 60m, underwater pipelines can be repaired by orbital GTAW, using cheap and readily available air as chamber gas to empty water [4, 5]. However, the stability of GTAW deteriorates quickly with the growing ambient pressure. The effects of GMAW on arc behavior, weld formation, and joint mechanics have been extensively researched [6, 7]. Although GMAW works stably under the pressure up to 25MPa, pulsed GMAW is a more feasible choice for underwater hyperbaric welding, because of its good controllability and adjustability [8-10]. Hyperbaric welding usually takes place in a large sealed chamber, in which the water is displaced by high-pressure gas to create a dry gas environment.

The weld quality directly depending on welding parameters. To improve weld quality, the key lies in the stability of welding arc [11]. Experimental results prove that the electrical

features of welding arc, namely, welding current, length of welding wire, and arc voltage, vary with the growing ambient pressure [12, 13]. During the welding process, welding current, arc voltage, pulse frequency, and the composition of shielding gas have great impact on the formation of molten pool and droplet, thereby affecting the welding stability [14, 15].

This paper builds a hyperbaric welding chamber to simulate the repair of subsea structures, and carries out welding tests under hyperbaric environment. In the light of the test results, the authors explored how pulsed GMAW parameters, such as arc voltage, peak current, base current, and pulse frequency, influence weld formation, and the microstructure of weld zone and heat-affected zone (HAZ). Besides, the mechanical performance of joints welded in hyperbaric environment was tested. On this basis, the welding parameters of pulsed GMAW were improved effectively.

2. HYPERBARIC WELDING TEST SYSTEM AND TEST METHOD

As shown in Figure 1, our hyperbaric welding test system mainly consists of a hyperbaric welding chamber (Figure 2), a welding head, and a welding power source. Specifically, the hyperbaric welding chamber is a horizontal pressure vessel designed to store 1MPa gases, with a door that can be closed and locked by hydraulic fluid. The three-axial welding head

realizes welding movements driven by servo motors, under the control of a welding control unit. It can be integrated in many welding processes, e.g. GTAW, GMAW, laser welding, and plasma arc welding. As shown in Figure 3, the welding head can be configured to meet specific position requirements. The

welding power source is set beside the hyperbaric welding chamber, and connected with the welding gun and workpiece via a special designed sealed component crossing flange on the chamber door.

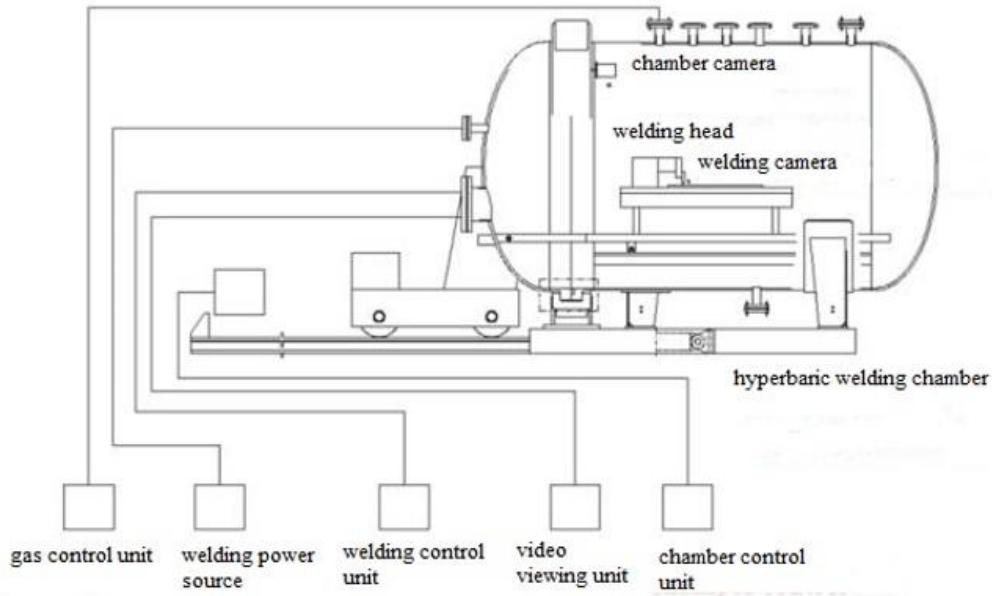


Figure 1. The structure of the hyperbaric welding test system

Table 1. The welding parameters

Test item	Arc voltage (V)	Average current (A)	Peak current (A)	Base current (A)	Pulse frequency (Hz)
No.1 Effect of arc voltage	28.8/31.8	200	480	70	190
No.2 Effect of peak current	28.8	200	480/500	70	190
No.3 Effect of base current	28.8	200	480	70/80	190
No.4 Effect of pulse frequency	28.8	200	480	70	190/220



Figure 2. The hyperbaric welding chamber



Figure 3. The welding head

To simulate the repair of subsea structure in hyperbaric environment, the chamber gases were filled and released by a gas control unit, using a computer program. During welding

operations, the scene of the chamber and the welding process were under video surveillance from the outside.

As shown in Figure 4, the test plate (L×W×H: 300mm×150mm×10mm) is a V-grooved Q345 steel plate. The welding tests adopt GB ER50-6 welding wires (diameter: 1.2mm), using a digital pulsed GMAW power source. The parameters of the power source, including peak current, arc voltage, pulse frequency, and base current, can be set independently and controlled precisely.

During the tests, only one of the parameters was changed at a time, aiming to disclose the influence of that specific parameter on weld formation, and the microstructure and mechanical performance of weld zone and HAZ. For example (No. 1 in Table 1), the arc voltage was set to 28.8 or 31.8V, while other parameters were kept constant, in order to investigate the impacts of arc voltage. In all welding tests, argon serves as the shielding gas, flowing at the rate of 20L/min.

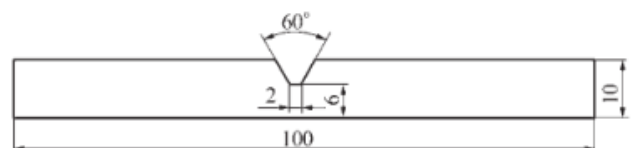


Figure 4. The groove of test plate

3. WELD FORMATION UNDER HYPERBARIC ENVIRONMENT

With the ambient pressure rising from 0.1 to 0.5MPa, a welding test was conducted at the arc voltage of 28.8V, with the other parameters configured as No.1 in Table 1. Figures 5 and 6 record the weld appearances and the macro-images of weld cross-section at different ambient pressures, respectively.

As the ambient pressure grew, more spatter loss and weld fume were observed, and the smooth weld surface under 0.1MPa changed into a rough surface under 0.5MPa (Figure 5). Meanwhile, the angle between metal liquid and basement surface shrunk with the increase of the arc force, which expands the weld width. In addition, the weld became shallower, due to the severe arc heat loss under hyperbaric environment (Figure 6).

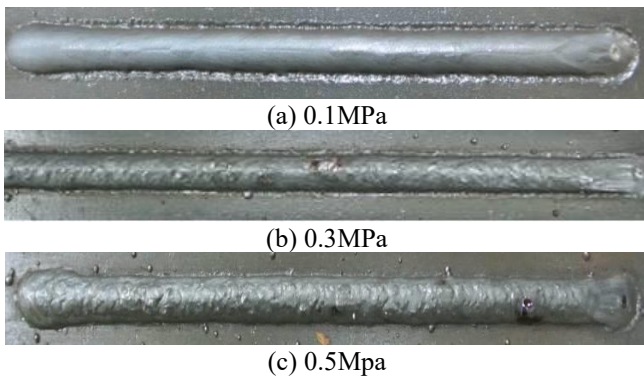


Figure 5. The weld appearances at different ambient pressures

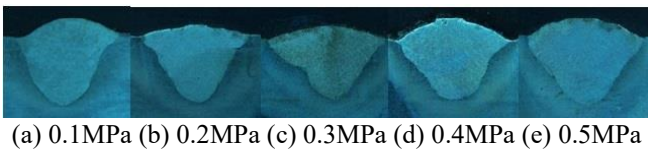


Figure 6. The macro-images of weld cross-section at different ambient pressures

4. EFFECTS OF ARC VOLTAGE ON WELD FORMATION AND MICROSTRUCTURE

The ambient pressure greatly suppresses the arc behavior, weld formation, and weld quality of pulsed GMAW in hyperbaric environment. The higher the ambient pressure, the more unstable the arc. Figure 7 presents the macro-images of weld cross-section at different arc voltages under 0.3MPa. Because of large heat loss under high ambient pressure, heat input to the molten pool became insufficient, resulting in the lack of fusion in Figure 7(a). As the arc voltage increased from 28.8 to 31.8V, more energy was supplied and a much better weld was formed in Figure 7(b). Therefore, when other parameters are fixed, the growing arc voltage could effectively compensate for the arc heat loss, improving arc stability and weld formation.

Figure 8 presents the microstructures of the weld zone at different arc voltages. When the arc voltage increased to 31.8V, a small amount of upper bainite appeared in the upper part of the weld zone, lots of grain boundary ferrites were distributed along the columnar grain boundaries, and a few low-carbon martensite was observed inside crystals. These can effectively

improve the tensile strength, plasticity, and toughness of the weld zone. The middle and bottom parts of the weld zone were composed of tempered martensite and fine cementite.

Figure 9 presents the microstructures of HAZ at different arc voltages. It can be seen that the microstructure of HAZ did not change much in the coarse grain zone. It mainly encompassed coarse austenite, a few bainite, and Widmanstätten structure on austenite grain boundaries. This means the cooling speed is high, and the coarse grain zone is crisp, reducing the mechanical performance of the joint.

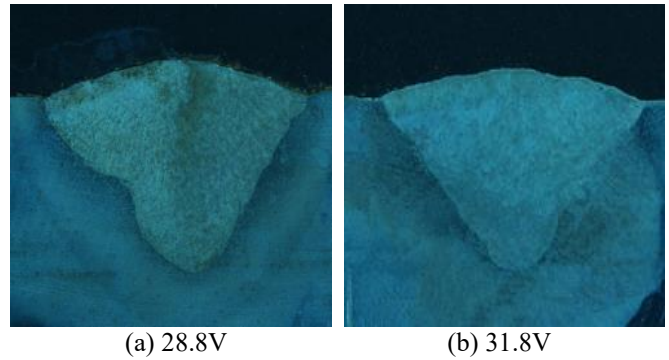


Figure 7. The macro-images of weld cross-section at different arc voltages under 0.3MPa

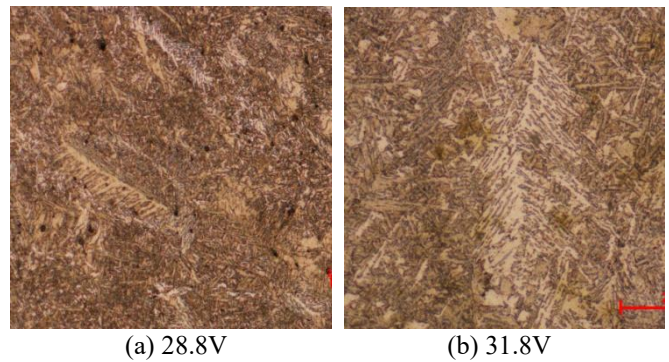


Figure 8. The microstructures of the weld zone at different arc voltages

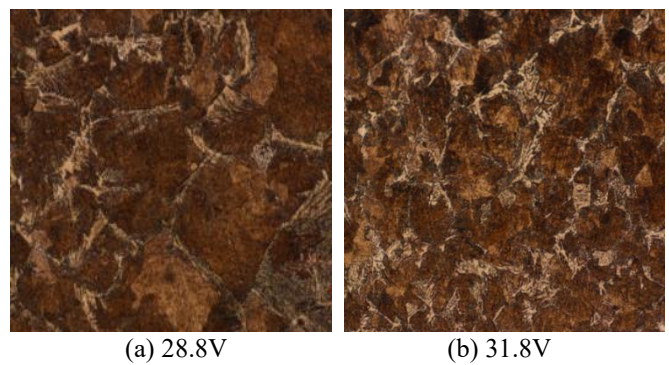


Figure 9. The microstructures of HAZ at different arc voltages

5. EFFECTS OF CURRENT ON WELD FORMATION AND MICROSTRUCTURE

Figure 10 presents the macro-images of weld cross-section at different peak currents under 0.3MPa. It can be seen that the porosity declined significantly, as the peak pulse current

increased from 480 to 500A. At the same average current, the growing peak pulse current could eliminate the drift of arc and strengthen the arc force, enhancing the stirring effect of arc on the molten pool. In addition, with the increase of the base current, better weld formation was also obtained, because weld wire and base metal are preheated in advance (Figure 11).

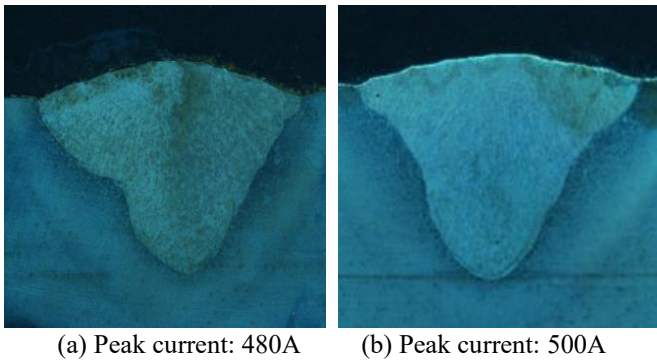


Figure 10. The macro-images of weld cross-section at different peak currents under 0.3MPa

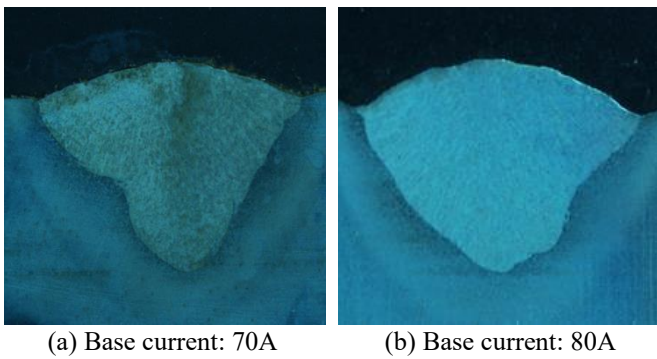


Figure 11. The macro-images of weld cross-section at different base currents under 0.3MPa

Figure 12 presents the microstructures of the weld zone at different peak currents. When the peak current was 480A, there were a lot of hard and brittle acicular martensite in the weld zone. After the peak current climbed up to 500A, the long eutectoid ferrite on the grain boundary was broken into massive ferrite, the content of granular bainite on the ferrite matrix was increased, and the crystal was composed of fine pearlite and acicular ferrite.

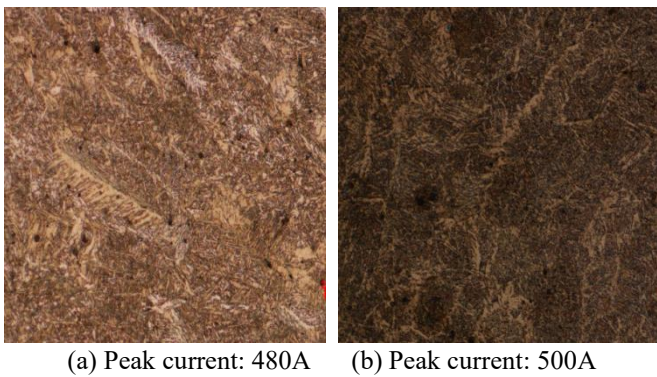


Figure 12. The microstructures of the weld zone at different peak currents

Figure 13 presents the microstructures of HAZ at different

peak currents. When peak current was 480A, the proeutectoid ferrite on the grain boundary of coarse austenite was mainly composed of upper bainite, forming a network structure. As the peak current increased from 480 to 500A, the coarse austenite grains were refined, and the microstructure was mainly made up of massive ferrite and fine pearlite. This improves the mechanical performance of HAZ.

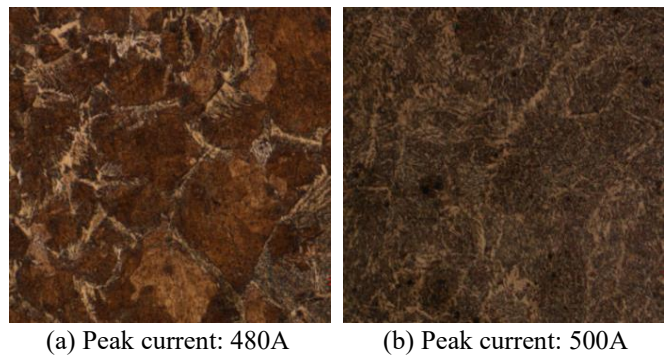


Figure 13. The microstructures of HAZ at different peak currents

Figure 14 presents the microstructures of the weld zone at different base currents. As the base current increased from 70A to 80A, there were still lots of ferrite on the coarse grain boundary in the weld zone, indicating that the microstructure of the weld zone is not much affected by the base current.

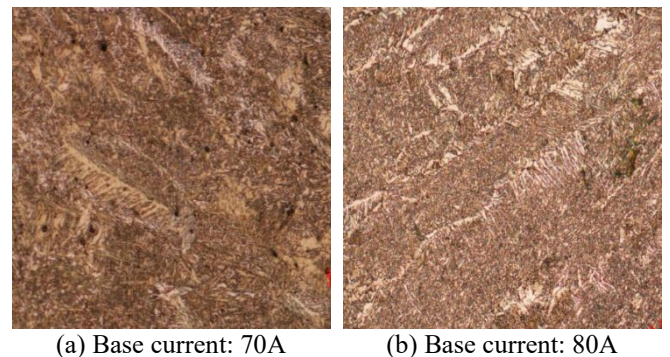


Figure 14. The microstructures of the weld zone at different base currents

Figure 15 presents the microstructures of HAZ at different base currents. As the base current increased from 70A to 80A, the coarse grain zone of the HAZ was refined, but the microstructure was not obviously optimized.

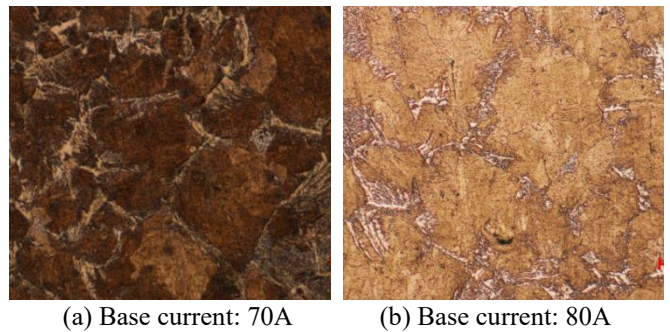


Figure 15. The microstructures of the HAZ at different base currents

6. EFFECTS OF PULSE FREQUENCY ON WELD FORMATION AND MICROSTRUCTURE

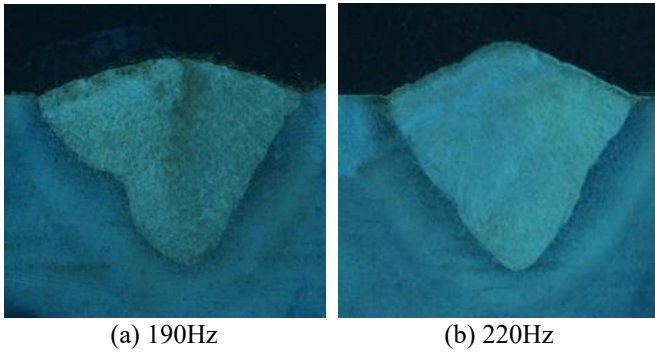


Figure 16. The macro-images of weld cross-section at different pulse frequencies under 0.3MPa

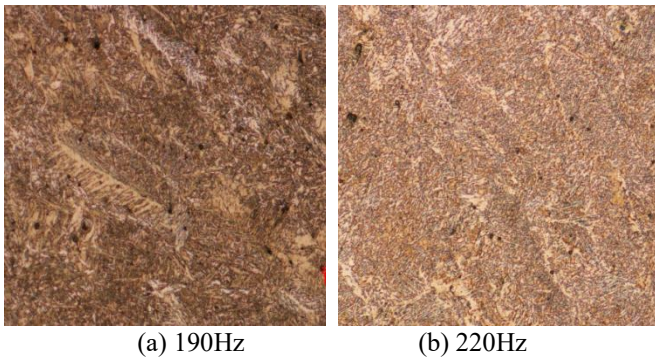


Figure 17. The microstructures of the weld zone at different pulse frequencies

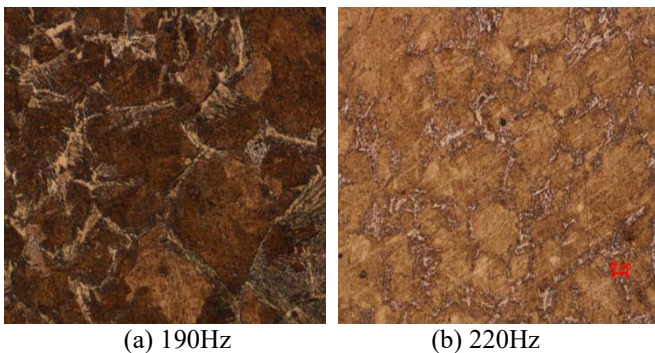


Figure 18. The microstructures of HAZ at different pulse frequencies

Figure 16 presents the macro-images of weld cross-section at different pulse frequencies under 0.3MPa. Comparing Figures 16(a) and 16(b), the increase of pulse frequency

improved arc energy and optimized the weld zone. With the increase of pulse frequency, arc column contracted and the pressure went up at the arc center. The large arc force led to big weld penetration. Furthermore, no porosity was observed in the weld zone at 220Hz, indicating that the arc heat loss at 0.3MPa is effectively compensated for by the rising pulse frequency.

Figure 17 presents the microstructures of the weld zone at different pulse frequencies. As the pulse frequency increased from 190 to 220Hz, granular pearlite, as the main component of microstructure, was refined. This is because the convection of liquid metal in the molten pool is improved by the rising pulse frequency, resulting in better fusion and grain refinement.

Figure 18 presents the microstructures of HAZ at different pulse frequencies. Despite the limited changes in the coarse grain zone, the size of austenite grains was greater at 190Hz than at 220Hz, and the amount of proeutectoid ferrite on austenite grain boundary increased as the pulse frequency changed from 190 to 220Hz.

7. MECHANICAL PERFORMANCE OF JOINTS WELDED UNDER HYPERBARIC ENVIRONMENT

7.1 Tensile strength of welding joints

Two groups of specimens were prepared for tensile strength tests. As shown in Table 2, the joints A1-3 in Group A were welded at 0.1, 0.3, and 0.5MPa, respectively, at the arc voltage of 28.8V, with other welding parameters the same as No.1 in Table 1; the joints B1-4 in Group B were welded under the same ambient pressure of 0.3MPa, at the arc voltage of 31.8V, the peak current of 500A, the base current of 80A, and the pulse frequency of 220Hz, while the other welding parameters were set as No.1 to No.4 in Table 1 in turn.

According to the *Tensile Test Method for Welding joints* (GB/T 2651-2008), the specimens were prepared with dimensions in Figure 19. Each type of specimen was subject to three repeated tests, and the average breaking load was obtained (Table 2). As shown in Figure 20, all specimens were broken at the position of the base metal, indicating that the weld zone has greater tensile strength than the base metal.

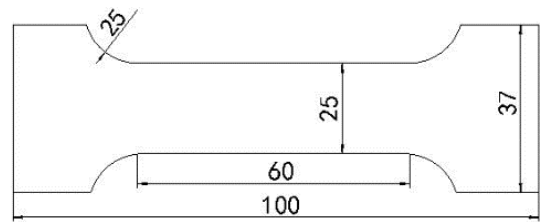


Figure 19. The dimensions of tensile specimens

Table 2. The results of tensile tests

Group	Specimen no.	Ambient pressure (MPa)	Welding parameters	Breaking load /N	Tensile strength /Rm	Breaking position
A	A1	0.1	Arc voltage=28.8V	51,484	515	Base material / brittle break
A	A2	0.3	Arc voltage=28.8V	50,620	506	Base material / brittle break
A	A3	0.5	Arc voltage=28.8V	49,654	497	Base material / brittle break
B	B1	0.3	Arc voltage=31.8V	51,032	510	Base material / brittle break
B	B2	0.3	Peak current=500A	49,665	493	Base material / brittle break
B	B3	0.3	Base current=80A	50,464	493	Base material / brittle break
B	B4	0.3	Pulse frequency=220Hz	50,620	506	Base material / brittle break



Figure 20. The broken specimens

7.2 Vickers hardness of welding joints

The Vickers hardness distribution of each welding joint was measured by an HVS-1000Z digital micro Vickers hardness tester under a load of 4.903N, which was maintained for 10 seconds. The test point was selected by the distance to the centerline of the specimen (Figure 21). As shown in Figure 22, the weld zone had the highest Vickers hardness, followed in turn by HAZ and base metal, regardless of the ambient pressure. It can also be learned that, with the increase of ambient temperature, the Vickers hardness of the weld zone generally increased, despite a few exceptions induced by the nonuniformity of the microstructure.

Figure 23 presents the distributions of Vickers hardness under 0.3 and 0.5MPa with the changing value of one of the welding parameters, such as arc voltage, peak current, base current, and pulse frequency. In other words, only one

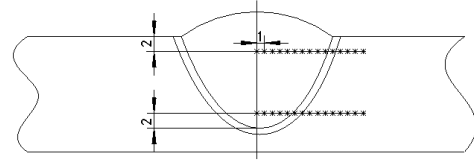


Figure 21. The test position of Vickers hardness

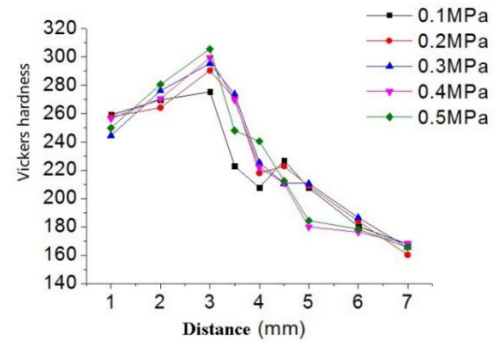
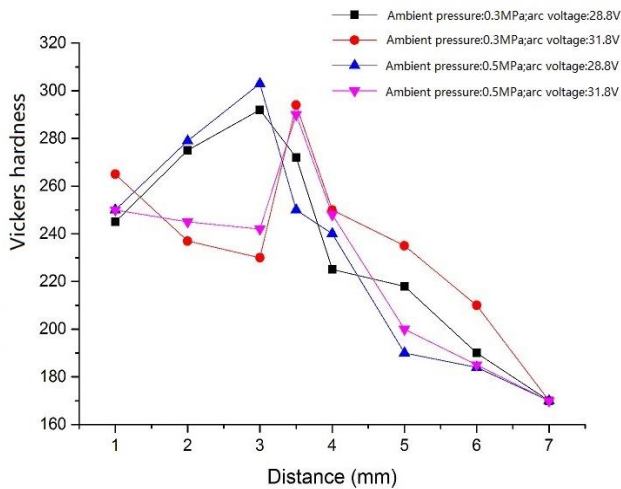
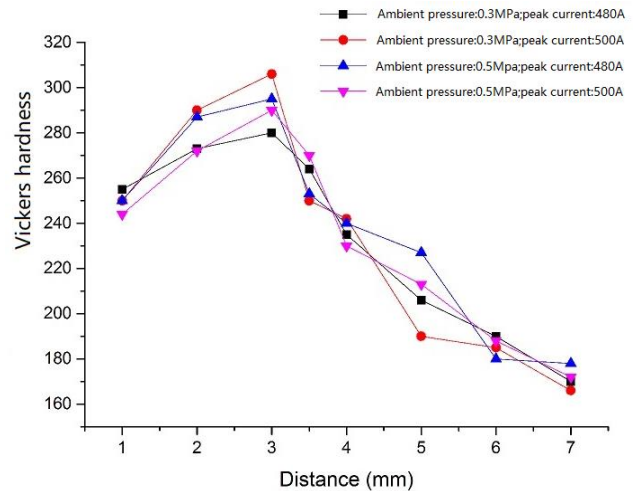


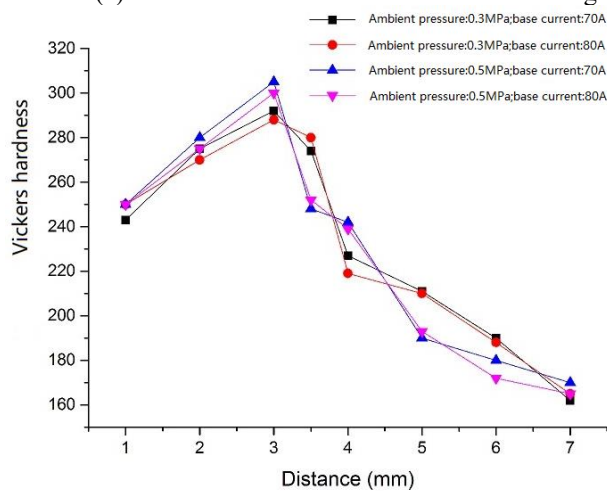
Figure 22. The effect of ambient pressure on weld hardness



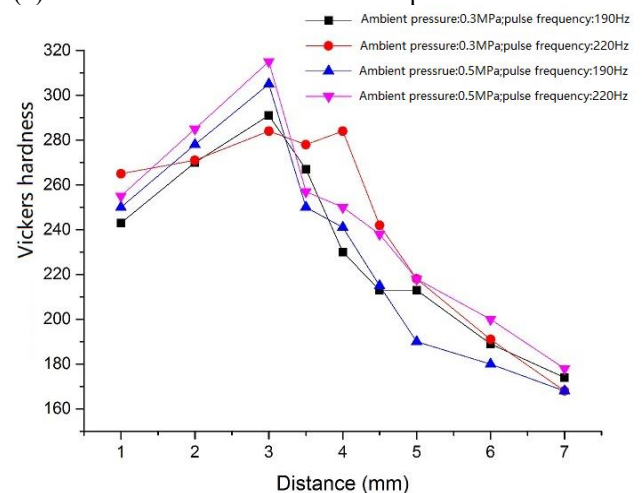
(a) Hardness distribution at different arc voltages



(b) Hardness distribution at different peak currents



(c) Hardness distribution at different base currents



(d) Hardness distribution at different pulse frequencies

Figure 23. The effects of welding parameters on weld hardness

Table 3. The results of Charpy impact tests

Group	Specimens no.	Ambient pressure (MPa)	Welding parameters	Impact power /N	Average power /N
A	A1	0.1	Arc voltage=28.8V	107, 105, 102	104.6
A	A 2	0.3	Arc voltage=28.8V	72, 70, 69	70.3
A	A 3	0.5	Arc voltage=28.8V	39, 42, 38	39.7
B	B 1	0.3	Arc voltage=31.8V	100, 89, 95	94.7
B	B 2	0.3	Peak current=500A	75, 68, 73	72
B	B 3	0.3	Base current=80A	72, 71, 68	70.3
B	B 4	0.3	Pulse frequency=220Hz	103, 95, 99	99

As shown in Figure 23(a), the Vickers hardness of HAZ increased, as the arc voltage was elevated from 28.8 to 31.8V. The rapid growth in hardness of HAZ is achieved, because the rising voltage widens the HAZ area, speeds up the cooling rate, and increases the occurrence of coarse austenite grains. Since the large number of ferrite needles are relatively fragile, the HAZ becomes much harder and less flexible. By contrast, the weld zone witnessed a decline of Vickers hardness and a rise in metal flexibility, as the arc voltage increased from 28.8 to 31.8V. This is attributable to the better microstructure supported by more heat input to the molten pool.

As shown in Figures 23(b) and 23(c), neither peak current nor base current had a significant impact on the Vickers hardness distribution of the welding joint. The function of peak current is to melt welding wire and base metal, while that of the base current is to maintain the pilot arc action. At the low arc voltage of 28.8V, the preheating of base metal and wire has little effect on the microstructure of the welding joint, owing to the limited amount of heat input. Similarly, when the arc voltage was at a low level, the increase of pulse frequency has little effect on the Vickers hardness distribution of the welding joint (Figure 23(d)).

7.3 Toughness of welding joints

For Charpy impact tests, several specimens were machined and sampled from the joints welded under the condition of Table 2 in Subsection 7.1. Then, Charpy impact tests were carried out at 20°C. The test results are displayed in Table 3 and Figure 20. As the ambient pressure was elevated from 0.1 to 0.5MPa, the weld toughness weakened due to the growing amount of upper bainite. The weld toughness could be improved at the arc voltage of 31.8V or the pulse frequency of 220Hz, but was not affected obviously by the adjustment of peak current or base current.

8. CONCLUSIONS

(1) Ambient pressure greatly suppresses the arc behavior, weld formation, and weld quality. The suppression could be effectively compensated for by elevating the arc voltage.

(2) The microstructures of weld zone and HAZ could be changed in varied degrees by adjusting welding parameters of GMAW, including arc voltage, peak current, base current, and pulse frequency.

(3) Ambient pressure also affects the mechanical performance of welding joints in terms of tensile strength, Vickers hardness and toughness. The mechanical performance could be improved by adjusting the welding parameters.

ACKNOWLEDGMENT

Supported by National Natural Science Foundation of

China (Grant No. 51675052).

REFERENCES

- [1] Zhou, C.F., Jiao, X.D., Xue, L., Chen, J.Q., Fang, X.M. (2011). Study on sub-sea pipelines hyperbaric welding repair under high air pressures. In *Robotic Welding, Intelligence and Automation*, 88: 391-397. https://doi.org/10.1007/978-3-642-19959-2_48
- [2] Nixon, J. (2000). *Underwater Repair Technology*. Cambridge: Woodhead Publishing Ltd., 2000.
- [3] Gao, H., Jiao, X.D., Xu, Y.G., Zhou, C.F. (2014). Study of underwater friction welding technology. *Welding Journal*, 93(9): 54-58.
- [4] Ozden, H. (2008). Underwater Welding in Hyperbaric Conditions. *Sea Technology*, 49(6): 52-54.
- [5] Zhou, C., Jiao, X., Xue, L., Chen, J., Huang, X. (2010). Study on automatic hyperbaric welding applied in sub-sea pipelines repair. In the *Twentieth International Offshore and Polar Engineering Conference*. International Society of Offshore and Polar Engineers, pp. 229-233.
- [6] Richardson, I.M., Nixon, J.H., Nosal, P., Hart, P., Billingham, J. (2000). Hyperbaric GMA welding to 2,500 m water depth. In *Joint International Conference ETC/OMAE 2000*, pp. 927-936.
- [7] Hart, P., Richardson, I.M., Nixon, J.H. (2001). The effects of pressure on electrical performance and weld bead geometry in high pressure GMA welding. *Welding in the World*, 45(11-12): 25-33.
- [8] Azar, A.S., Ås, S.K., Akselsen, O.M. (2013). Analytical modeling of weld bead shape in dry hyperbaric GMAW using Ar-He chamber gas mixtures. *Journal of Materials Engineering and Performance*, 22(3): 673-680. <https://doi.org/10.1007/s11665-012-0331-z>
- [9] Xue, L., Wu, J., Huang, J., Huang, J., Zou, Y., Liu, J. (2016). Welding polarity effects on weld spatters and bead geometry of hyperbaric dry GMAW. *Chinese Journal of Mechanical Engineering*, 29(2): 351-356. <https://doi.org/10.3901/CJME.2015.1104.131>
- [10] Azar, A.S., Akselsen, O.M., Fostervoll, H. (2012). Prediction of the thermal cycles in dry hyperbaric GMA welding using partial differential heat transfer equations. In *Proceedings of the 9th International Conference, Trends in Welding Research*, Chicago, IL, USA. pp. 4-8.
- [11] Azar, A.S., Woodward, N., Fostervoll, H., Akselsen, O.M. (2012). Statistical analysis of the arc behavior in dry hyperbaric GMA welding from 1 to 250 bar. *Journal of Materials Processing Technology*, 212(1): 211-219. <https://doi.org/10.1016/j.jmatprotec.2011.09.006>
- [12] Azar, A.S., Lange, H.I., Østby, E., Akselsen, O.M. (2012). Effect of hyperbaric gas composition on mechanical properties of the weld metal. *Materials*

- Science and Engineering: A, 556: 465-472.
<https://doi.org/10.1016/j.msea.2012.07.013>
- [13] Akselsen, O.M., Fostervoll, H., Ahlen, C.H. (2009). Hyperbaric GMA welding of duplex stainless steel at 12 and 35 bar. *Welding Journal*, 88(2): 21-28.
- [14] Akselsen, O.M., Fostervoll, H., Ahlen, C.H. (2008). Hyperbaric gas metal arc welding of API X65 pipeline steel at 12, 25 and 35 bar. In the Eighteenth International Offshore and Polar Engineering Conference. International Society of Offshore and Polar Engineers, 20(2): 110-117.
- [15] Huang, J., Xue, L., Lv, T., Jiang, L. (2010). Experiment on characteristics of GMAW arc in underwater hyperbaric air condition. *Transactions of the China Welding Institution*, 31(12): 17-16.

ABBREVIATIONS

GMAW — Gas Metal Arc Welding
GTAW — Gas Tungsten Arc Welding
HAZ — Heat Affected Zone